



*Supplement of*

## **Image classification of marine-terminating outlet glaciers in Greenland using deep learning methods**

**Melanie Marochov et al.**

*Correspondence to:* Patrice E. Carbonneau ([patrice.carbonneau@durham.ac.uk](mailto:patrice.carbonneau@durham.ac.uk))

The copyright of individual parts of the supplement might differ from the article licence.

**Table S1: Descriptions of each of the seven semantic classes used to train the phase one CNN in the deep learning workflow. Example image samples of each class can be found in Fig. 2.**

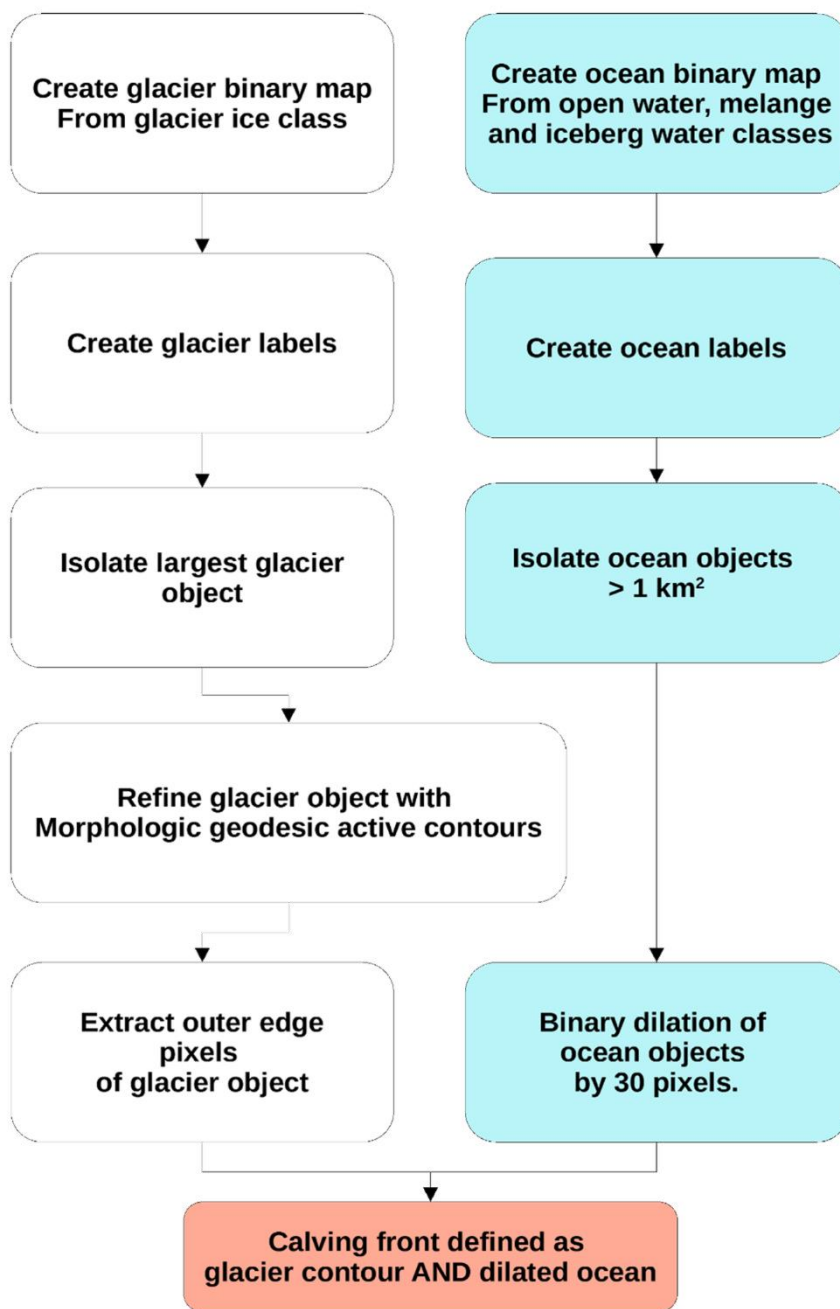
Class	Class description
1. <b>Open water</b>	Open water with no icebergs
2. <b>Iceberg water</b>	Water with varying amounts of icebergs or disintegrated mélange/sea-ice
3. <b>Mélange</b>	Mixture of sea-ice and icebergs of varying sizes
4. <b>Glacier ice</b>	Glacier ice, with seasonally variable surface meltwater
5. <b>Snow on ice</b>	Snow/ice with a smooth appearance
6. <b>Snow on rock</b>	Bedrock with varying amounts of snow cover
7. <b>Bedrock</b>	Bedrock with no snow cover

5

**Table S2: List of Sentinel-2 images used for training and testing the CSC workflow. Images with \* in the test dataset were removed from the validation of classifications which used the Joint training method as these images were used to fine tune the phase one CNN.**

Study Area		Acquisition Date	Scene Filename
<b>Helheim</b>	<b>Training</b>	8 Feb 2019	S2A_MSIL2A_20190208T142341_N0211_R096_T24WWU_20190208T144632
		10 Feb 2019	S2B_MSIL2A_20190210T141329_N0211_R053_T24WWU_20190210T163824
		7 March 2019	S2A_MSIL2A_20190307T141031_N0211_R053_T24WWU_20190307T145436
		10 March 2019	S2A_MSIL2A_20190310T142011_N0211_R096_T24WWU_20190310T151039
		15 March 2019	S2B_MSIL2A_20190315T141949_N0211_R096_T24WWU_20190315T183613
		4 April 2019	S2B_MSIL2A_20190404T141739_N0211_R096_T24WWU_20190404T171335
		29 May 2019	S2A_MSIL2A_20190529T141951_N0212_R096_T24WWU_20190529T183516
		15 June 2019	S2A_MSIL2A_20190615T141011_N0212_R053_T24WWU_20190615T145742
		5 July 2019	S2A_MSIL2A_20190705T141011_N0212_R053_T24WWU_20190705T180815
		07 August 2019	S2A_MSIL2A_20190807T142001_N0213_R096_T24WWU_20190807T151033
		01 September 2019	S2B_MSIL2A_20190901T141739_N0213_R096_T24WWU_20190901T165620
		28 September 2019	S2B_MSIL2A_20190928T140949_N0213_R053_T24WWU_20190928T150105
26 October 2019	S2A_MSIL2A_20191026T142301_N0213_R096_T24WWU_20191026T144852		

<b>cont.</b>	<b>Testing</b>	5 March 2019*	S2B_MSIL2A_20190305T142049_N0211_R096_T24WWU_20190305T200258
		9 April 2019	S2A_MSIL2A_20190409T141951_N0211_R096_T24WWU_20190409T165416
		26 May 2019	S2A_MSIL2A_20190526T141011_N0212_R053_T24WWU_20190526T150051
		5 June 2019	S2A_MSIL2A_20190605T141011_N0212_R053_T24WWU_20190605T182225
		18 June 2019	S2A_MSIL2A_20190618T141951_N0212_R096_T24WWU_20190618T181858
		8 July 2019	S2A_MSIL2A_20190708T142001_N0213_R096_T24WWU_20190708T150305
		17 August 2019	S2A_MSIL2A_20190817T141951_N0213_R096_T24WWU_20190817T181715
		13 September 2019	S2A_MSIL2A_20190913T141001_N0213_R053_T24WWU_20190913T150142
		1 October 2019*	S2B_MSIL2A_20191001T142009_N0213_R096_T24WWU_20191001T165936
<b>Jakobshavn</b>		21 April 2020*	S2A_MSIL2A_20200421T151911_N0214_R068_T22WEB_20200421T175937
		8 May 2020	S2A_MSIL2A_20200508T150921_N0214_R025_T22WEB_20200508T191808
		21 May 2020	S2A_MSIL2A_20200521T151921_N0214_R068_T22WEB_20200521T175842
		1 June 2019*	S2B_MSIL2A_20190601T151809_N0212_R068_T22WEB_20190601T190621
		12 June 2020	S2B_MSIL2A_20200612T150759_N0214_R025_T22WEB_20200612T193002
		27 June 2020	S2A_MSIL2A_20200627T150921_N0214_R025_T22WEB_20200627T174250
		17 July 2020	S2A_MSIL2A_20200717T150921_N0214_R025_T22WEB_20200717T174337
<b>Store</b>		21 August 2020	S2B_MSIL2A_20200821T150809_N0214_R025_T22WEB_20200821T175633
		24 April 2020*	S2A_MSIL2A_20200424T152911_N0214_R111_T22WED_20200424T192351
		31 May 2020	S2A_MSIL2A_20200531T151921_N0214_R068_T22WED_20200531T193340
		28 June 2020	S2B_MSIL2A_20200628T152809_N0214_R111_T22WED_20200628T194322
		20 July 2020	S2A_MSIL2A_20200720T151911_N0214_R068_T22WED_20200720T175341
		2 August 2020*	S2A_MSIL2A_20200802T152911_N0214_R111_T22WED_20200802T181251
		22 August 2020	S2A_MSIL2A_20200822T152911_N0214_R111_T22WED_20200822T194838
		30 August 2020	S2B_MSIL2A_20200830T153819_N0214_R011_T22WED_20200830T180413
		14 September 2020	S2A_MSIL2A_20200914T153911_N0214_R011_T22WED_20200914T201155
		23 September 2020	S2B_MSIL2A_20200923T151849_N0214_R068_T22WED_20200923T194810
8 October 2020		S2A_MSIL2A_20201008T152141_N0214_R068_T22WED_20201008T175852	



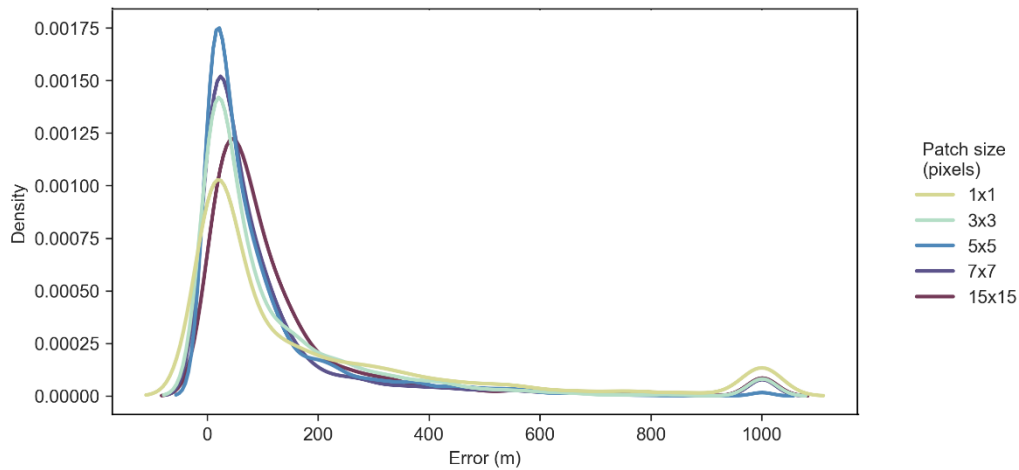
15 **Figure S1: Flowchart for calving front detection algorithm. The algorithm starts with the glacier ice class and then defines an ‘Ocean’ class by combining the open water, mélange and iceberg water classes. Then a series of binary morphology operations, including geodesic active contours, are used to define the calving front as the intersection (boolean AND) of a refined glacier outer edge and a dilated ocean object.**

20

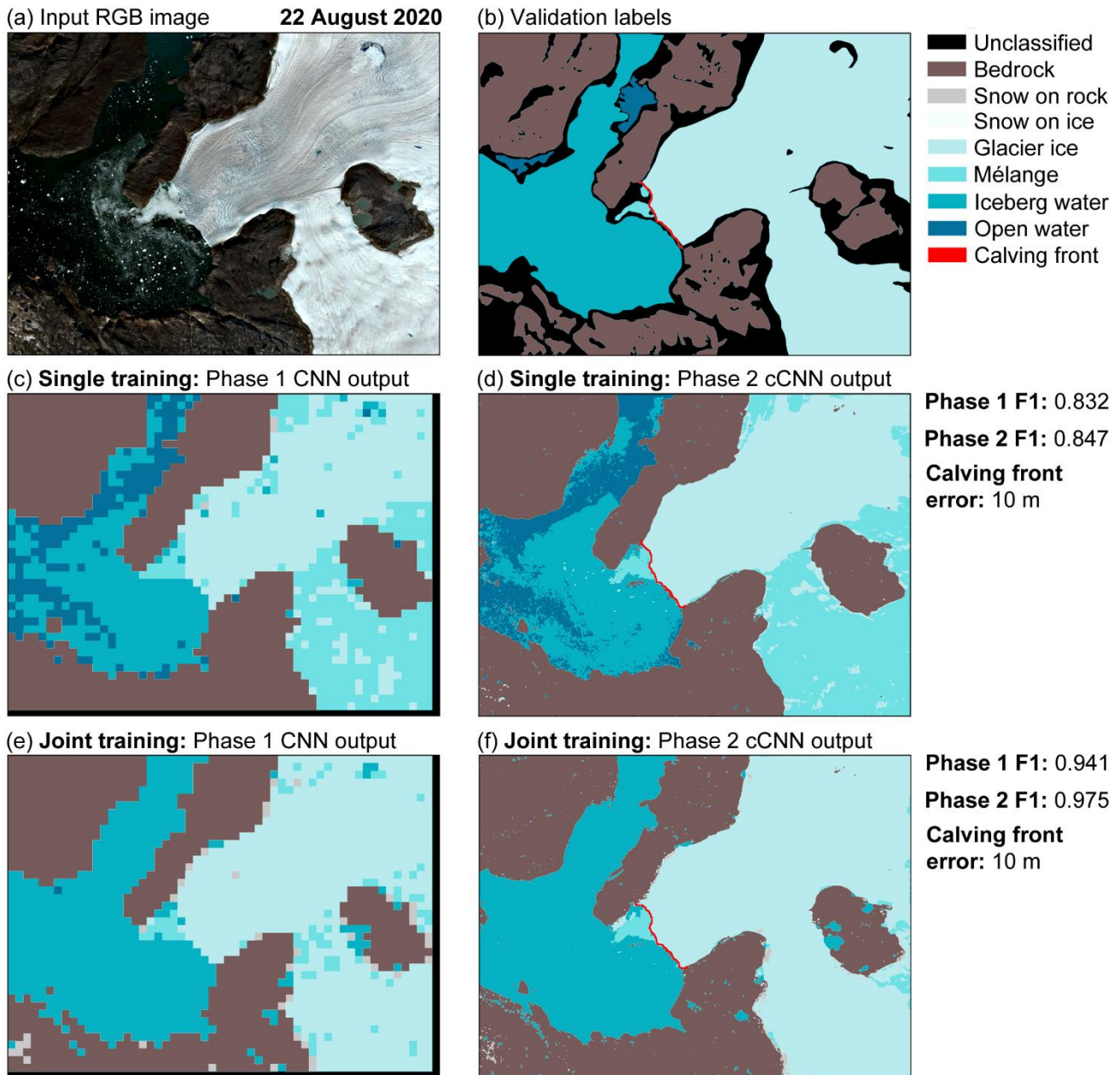
25 **Table S3: Phase one F1 scores within the given parameters of tile size and band combinations. Highest values are highlighted in bold for in-sample and out-of-sample test imagery. Note that in both cases, using 50x50 RGBNIR tiles produces optimal results.**

Phase 1 F1 scores (%)	In-sample			Out-of-sample		
	Tile size (pixels)					
	50x50	75x75	100x100	50x50	75x75	100x100
<b>RGB bands</b>	91.1	90.7	89	83.3	86.4	89.3
<b>RGBNIR bands</b>	<b>92.2</b>	90	88.3	<b>89.7</b>	87.3	86.5

30



35 **Figure S2: A kernel density estimate (KDE) plot of the full error distribution for all calving front predictions derived from all test sites using classifications produced with optimal parameters and Joint training. Error values above 1000 m are grouped into a single bin to reduce tail length and show a second peak which represents catastrophic errors in calving front prediction. Note that low calving front errors occur most with 5x5 patches, followed by 7x7 and 3x3 patches, with highest error occurring for the pixel-based approach.**

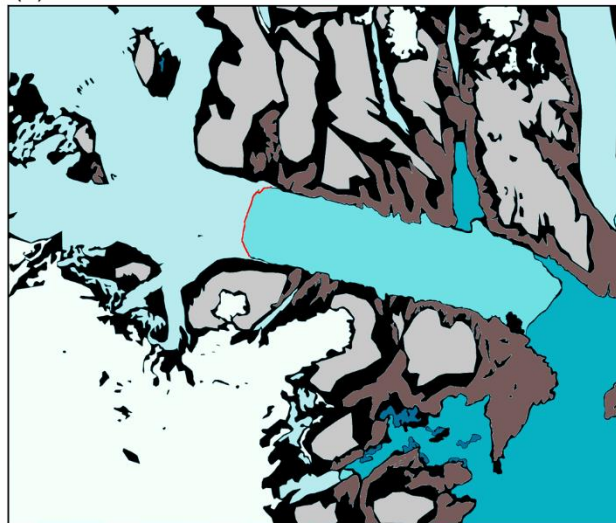


40 **Figure S3: Comparison of Single and Joint training methods for (a) an image of Store glacier acquired on 22 August 2020. (b)**  
**shows the manually collected validation labels. (c) Shows the phase one tiled output using Single training and (d) shows the**  
**resulting CSC output. Note the area of glacier ice which has been misclassified using Single training. (e) Shows the phase one**  
**output using Joint training with the associated pixel-level phase two output shown in (f). A tile size of 50x50 pixels, patch size of**  
**5x5 pixels and RGBNIR bands were used in the examples shown here. The Joint training method rectifies the misclassified area of**  
 45 **glacier ice. All Sentinel-2 imagery in this figure has been made available courtesy of the European Union Copernicus program.**

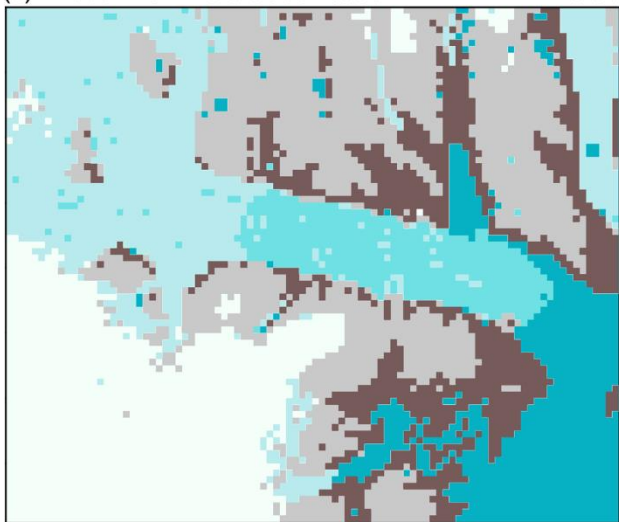
(a) Input RGB image Helheim 18 June 2019



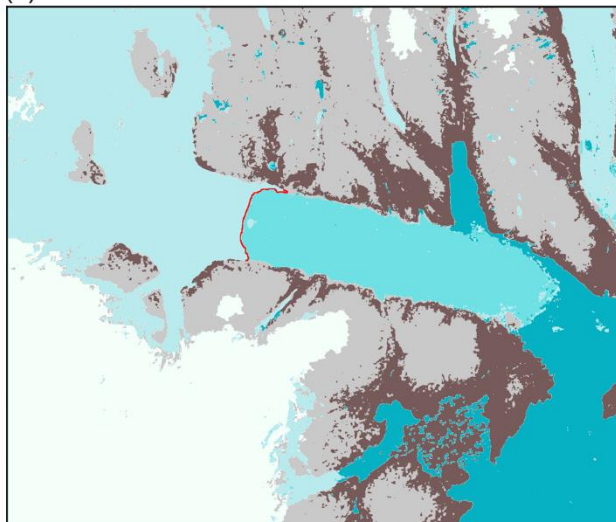
(b) Validation labels



(c) Phase 1 CNN tile classification F1: 0.93



(d) Phase 2 cCNN classification F1: 0.949

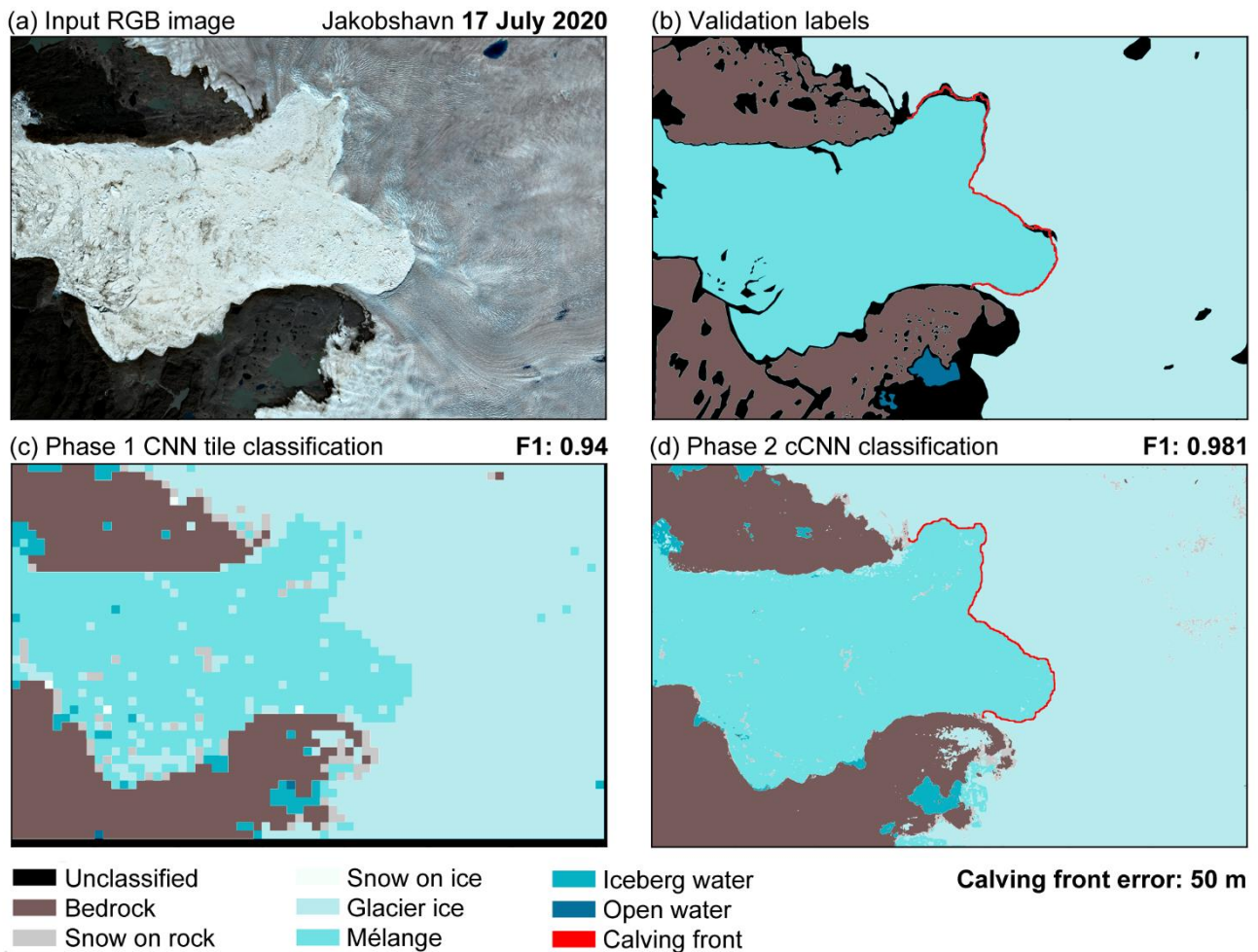


Legend for classification results:

■ Unclassified	■ Snow on ice	■ Iceberg water
■ Bedrock	■ Glacier ice	■ Open water
■ Snow on rock	■ Mélange	■ Calving front

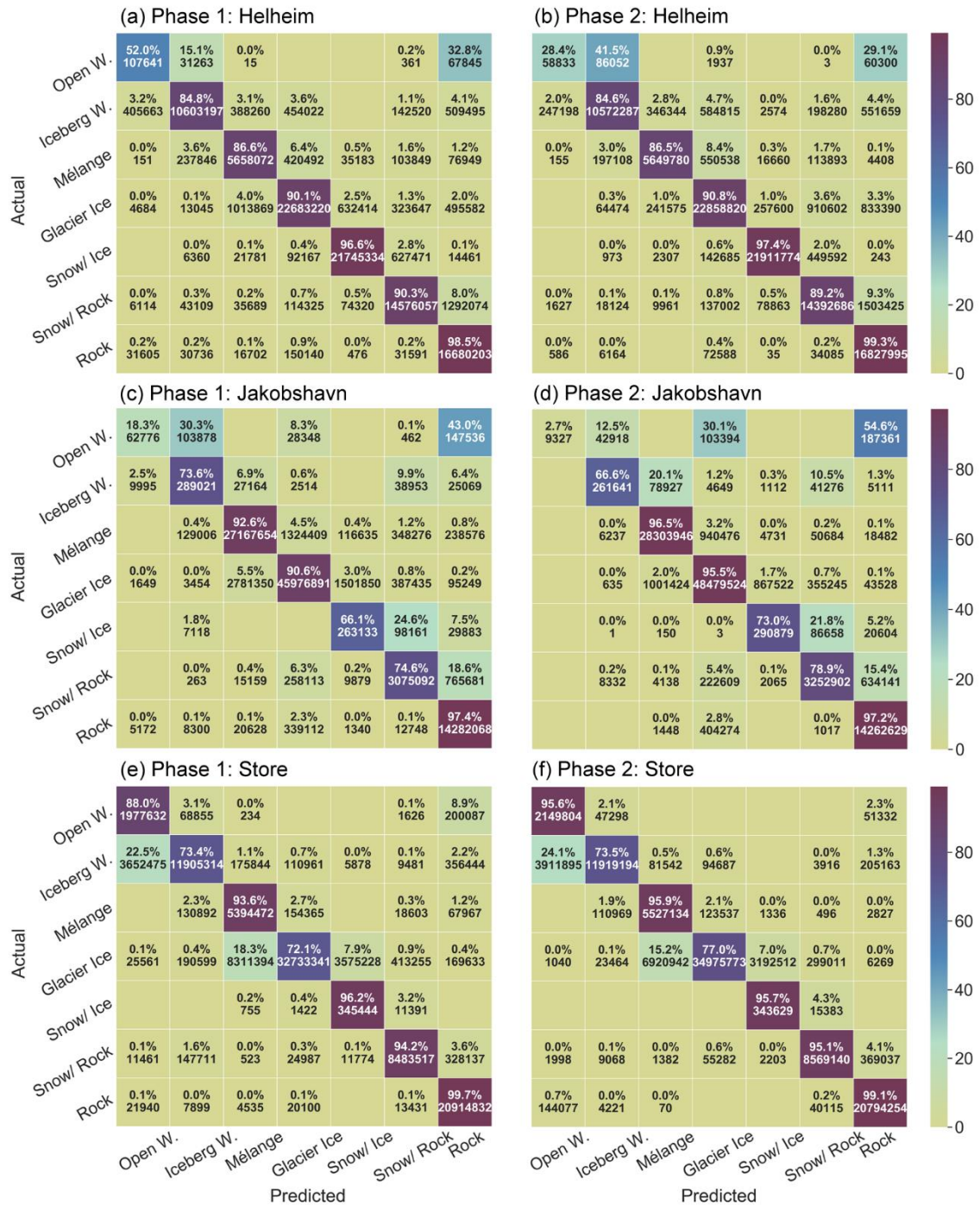
Calving front error: 50 m

Figure S4: Example of CSC using Joint training for (a) an unseen image of Helheim acquired on 18 June 2019. (b) Shows the manually collected validation labels. (c) Shows the tiled output of the phase 1 CNN and (d) shows the final pixel-level classification with an associated calving front detection. The optimum classification parameters were used in this example. All Sentinel-2 imagery in this figure has been made available courtesy of the European Union Copernicus program.



55 **Figure S5: Example of CSC using Joint training for (a) an unseen image of Jakobshavn acquired on 17 July 2020. (b) Shows the manually collected validation labels. (c) Shows the tiled output of the phase 1 CNN and (d) shows the final pixel-level classification with an associated calving front detection. The optimum classification parameters with a tile size of 50, patch size of 5 and RGBNIR bands were used in this example. All Sentinel-2 imagery in this figure has been made available courtesy of the European Union Copernicus program.**

60



**Figure S6: Confusion matrices for CSC results using Single training with optimal parameters for each glacier. Showing the confusion between predicted and true classes for the Helheim site in (a) phase one and (b) phase two classifications, for Jakobshavn in (c) phase one and (d) phase two, and for Store in (e) phase one and (f) phase two. Note that the only significant confusion occurs for the open water class for Helheim and Jakobshavn. Matrices produced using 100 million subsamples of the full results from each glacier.**

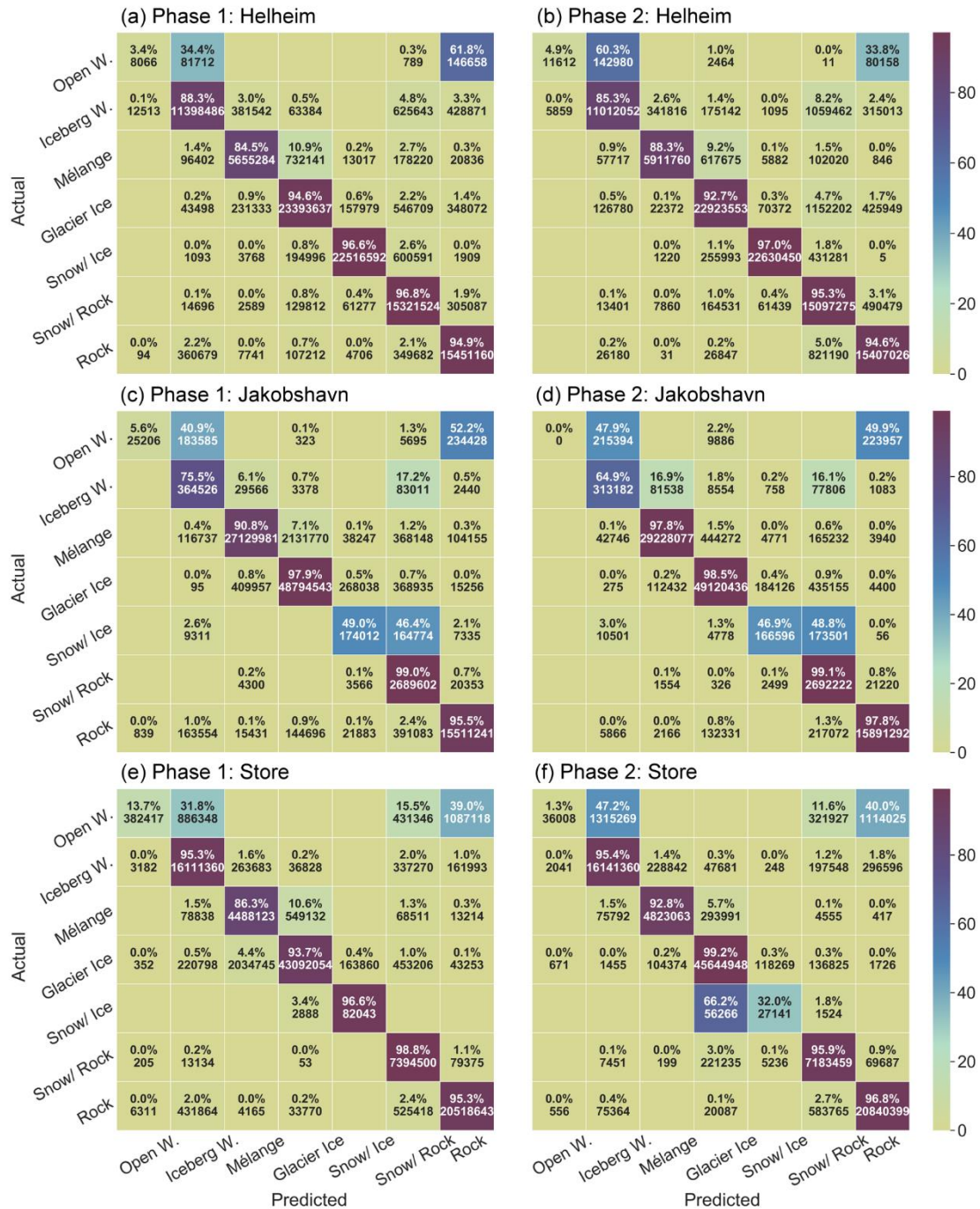
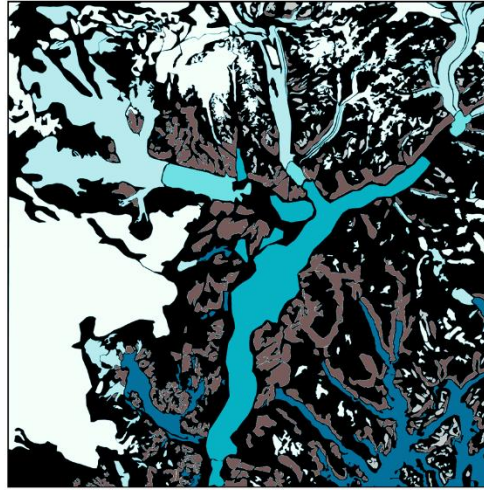


Figure S7: Confusion matrices for CSC results using Joint training with optimal parameters for each glacier. Showing the confusion between predicted and true classes for the Helheim site in (a) phase one and (b) phase two classifications, for Jakobshavn in (c) phase one and (d) phase two, and for Store in (e) phase one and (f) phase two. Note that the pattern of inter-class confusion differs to that of Single training, but overall F1s are higher. Matrices produced using 100 million subsamples of the full results from each glacier

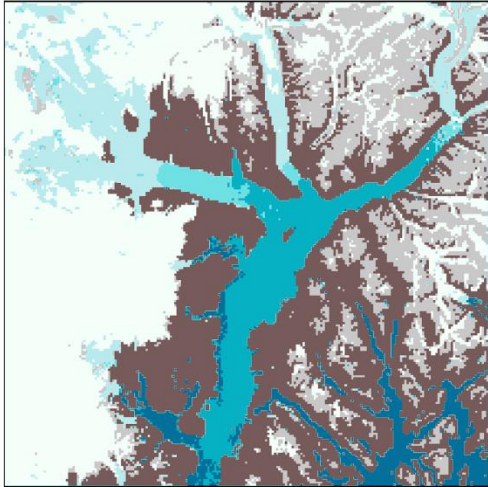
(a) Input Sentinel-2 tile 13 September 2019



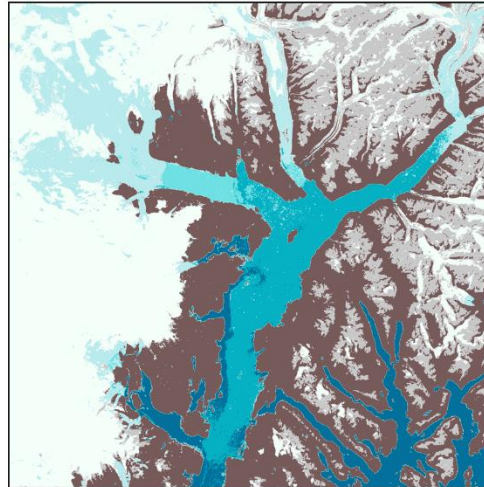
(b) Validation labels



(c) Phase 1 CNN tile classification F1: 0.911



(d) Phase 2 cCNN classification F1: 0.92



75 **Figure S8: CSC performance on (a) an entire Sentinel-2 tile. (b) Shows validation labels. (c) Shows the tiled classification output of phase one which was used as the training labels in phase two, producing a final pixel-level classification shown in (d). The final classification was produced using RGBNIR tiles with a size of 50x50 pixels and a cCNN patch size of 7x7 pixels using Single training. The Sentinel-2 imagery in this figure has been made available courtesy of the European Union Copernicus program.**